The $p^3 \otimes h$ Jahn–Teller effect in a distorted environment

2005 J. Phys.: Condens. Matter 17 5499

(http://iopscience.iop.org/0953-8984/17/36/006)

INSTITUTE OF PHYSICS PUBLISHING JOURNAL OF PHYSICS: CONDENSED MATTER

J. Phys.: Condens. Matter **17** (2005) 5499–5516 doi:10.1088/0953-8984/17/36/006

The $p^3 \otimes h$ Jahn–Teller effect in a distorted environment

Janette L Dunn

School of Physics and Astronomy, University of Nottingham, University Park, Nottingham NG7 2RD, UK

E-mail: Janette.Dunn@nottingham.ac.uk

Received 23 June 2005
Published 26 August 2005
Online at stacks.iop.org/JPhysCM/17/5499

Abstract

The behaviour of isolated fullerene anions C_{60}^{3-} can be strongly influenced by coupling to intramolecular modes of vibration of the C_{60} molecule, which can be described by a $p^3 \otimes h$ Jahn–Teller (JT) effect. In solids such as the A_3C_{60} fullerides, the ions are also coupled to intermolecular vibrational modes resulting in a cooperative JT effect. Dynamic distortions of individual ions can be locked in place resulting in a static distortion of the solid as a whole. The effect of the distortion on an individual ion can be modelled by introducing a net strain into the basic $p^3 \otimes h$ JT effect. In this paper, we will determine analytical expressions for the eigenstates and energies of this strained JT system, and evaluate the results numerically as functions of the JT coupling strength, the magnitude of the strain and the size of the splitting between different molecular terms.

(Some figures in this article are in colour only in the electronic version)

1. Introduction

It is well known that isolated C_{60} fullerene molecules have icosahedral (I_h) symmetry, and that the electrons in the valence orbitals of these fullerene molecules are strongly coupled to h_g-type vibrations of the molecular cage. For C_{60} anions and cations, which have degenerate electronic ground states, the coupling results in a local distortion of the molecule into a configuration with a symmetry lower than I_h. However, there is a set of equivalent lower-symmetry configurations, and the system will tunnel between these configurations on a very rapid timescale. EPR data [1] suggest the tunnelling will take place in a time of the order of picoseconds, and estimates from the strengths of the vibronic coupling [2–6] and the tunnelling splitting between the lowest energy levels suggests a timescale of the order of femtoseconds. The tunnelling restores the overall I_h symmetry of the molecule for measurements on a longer timescale than this, in what is known as a dynamic Jahn–Teller (JT) effect.

The effect of vibronic coupling can be rather different in fullerene-based solids to that in isolated molecules. In this case, the distortion of a given molecule can be locked in place by distortions of its neighbouring molecules in a cooperative JT effect [7–9], which can result in a net overall distortion at low temperatures. This in turn can lead to different structural, orientational and magnetic phases [10]. Such a situation is known to occur in fullerene-based solids. For example, a structure that is likely to result in ferromagnetic order in TDAE-C_{60} has been presented by Kawamoto and co-workers [11, 12]. Further evidence for symmetry-lowering in fullerene anions comes from the ESR work of Kato and co-workers, who suggest a distortion to C_{2h} or C_i symmetry [13, 14]. As the temperature increases, thermal effects tend to destroy the correlations between the JT distortions at different lattice sites, and structural phase transitions may take place.

As a cooperative JT effect results in a net distortion, the effect on a given ion can be modelled by adding strain into models for JT effects in an isolated ion [15]. In this paper, we will specifically consider the effect of strain in JT systems applicable to C_{60}^{3-} anions, where the coupling is between electrons in p orbitals and h_g-type vibrations in what is known as the $p^3 \otimes h$ JT effect [16, 17]. C_{60}^{3-} ions occur in, for example, the A_3C_{60} fullerides, which can be superconducting at relatively high temperatures [18] as well as exhibiting orientational phase transitions from an unordered state to one with a mixture of two standard orientations (known as merohedral disorder) [19]. Our results may be of use in helping to interpret the vibronic spectrum of C_{60}^{3-} ions from spectroscopic experiments, and they can be used in further calculations such as investigations of cooperative JT effects in the A_3C_{60} solids.

Physically, the motion of any JT system can be understood by analysing the lowest adiabatic potential energy surface (APES) formed from the vibrational and JT potential energy terms combined with the effect of any splitting between different molecular terms. The precise structure of the APES depends on the order to which the JT coupling is taken. For many purposes it is sufficient to consider linear coupling only, even though for all of the $p^n \otimes h$ systems (applicable to C_{60}^{n-} ions) this results in an accidentally higher symmetry of SO(3) rather than I_h [16, 17, 20], as proved in general terms by Pooler [21].

For the unstrained $p^3 \otimes h$ JT system, the lowest APES is a five-dimensional surface containing a trough of equivalent minimum-energy points in three directions in linear coupling. As there are no barriers to motion in these directions, any distortion will rotate about these directions. This is known as a pseudo-rotation, to distinguish it from an actual rotation of the molecule itself. When the JT coupling is sufficiently strong, there are barriers restricting motion in the remaining two directions which result in local vibrations alongside the rotations in the other three directions. When a uniaxial strain is included, we will show that the APES distorts so that there is only a two-dimensional circle of equivalent minimum-energy points, leading to pseudo-rotation in one direction instead of three. The APES is warped in the remaining two directions to give wells whose depth increase as the strength of the strain increases.

The basic formalism we will use for writing down the Hamiltonian for the unstrained $p^3 \otimes h$ JT system and dividing the motion into vibrations and pseudo-rotations follows the original work of Auerbach *et al* [20], which was then further developed by O'Brien [16, 17]. We will then include an additional strain term in the Hamiltonian. Also, whereas these previous works used a numerical diagonalization to determine the energies of the rovibronic states, we will use an analytical approach to write down expressions for the energies and states in terms of integrals over the circle of minimum-energy points on the APES. We will show that it is important to take into account the effects of anisotropy in the APES, as the barrier heights and hence the vibrational frequencies will be much lower in the directions that correspond to rotations in the absence of strain than in the directions that always correspond to vibrations. To determine the energies of the states it is necessary to evaluate the integrals numerically.

However, as the integrals are only one dimensional, they can easily be evaluated by standard means. This is in contrast to the undistorted case, where the corresponding integrals are five dimensional and numerical problems were found to occur in evaluating the multi-dimensional integrals in some cases, as discussed in our previous work on both this system [22] and the $p^2 \otimes h$ system [23].

2. The Hamiltonian

An electronic configuration p^3 results in electronic terms ^4S, ^2D and ^2P [16, 17]. There is no JT coupling to the S state, and so it need not be considered any further here. It is also found that there is no JT coupling within either the ^2D or the ^2P states as all the required matrix elements are zero, and thus the only coupling that needs to be considered is coupling between the ^2P and ^2D states involving h_g vibrational modes [16, 17] (which is therefore known as a pseudo-JT problem). This was discussed in terms of quasi-spin quantization by Ceulemans [24].

Building upon previous approaches for the unstrained system [16, 17, 22], we will write the total Hamiltonian for the strained $p^3 \otimes h$ JT system in the form

$$\mathcal{H} = \mathcal{H}_{\text{int}} + \mathcal{H}_{\text{vib}} + \mathcal{H}_{\text{term}} + \mathcal{H}_{\text{strain}} \tag{1}$$

where $\mathcal{H}_{\text{int}}$ represents the JT interaction, $\mathcal{H}_{\text{vib}}$ represents the vibrational terms, $\mathcal{H}_{\text{term}}$ any splitting between the ^2P and ^2D terms and $\mathcal{H}_{\text{strain}}$ the effect of a strain along a given axis. C_{60} ions are coupled to eight h_g modes of frequencies ranging from around 260 to 1500 cm^{-1} [25]. However, for many purposes it is sufficient to consider coupling to a single mode represented by an effective frequency [26, 27], or coupling to the strongest mode only. We will therefore consider linear coupling to a single h_g mode. This will give a good indication of the effects of vibronic coupling in C_{60}^{3-} ions, although it may be necessary to include both higher-order couplings and the effects of multiple modes in order to explain the behaviour of these ions in detail.

In order to write down a more explicit form for $\mathcal{H}$, we need to define some notation for the collective coordinates of the h_g mode. In common with [22], we will use the labels $\{Q_\theta, Q_\epsilon, Q_4, Q_5, Q_6\}$, which correspond to the labels $\{Q_1, Q_4, Q_5, Q_2, Q_3\}$ used in [16] and [17]. Also, as mentioned above, the JT Hamiltonian is accidentally SO(3) invariant in linear coupling [21]. As a result, we only need to consider a strain in one specific direction. For convenience, we will choose to consider strains in the Q_θ coordinate. The results can then be used to model a strain in any direction. Mathematically, this is because a transformation of coordinates [38], combined with a rotation of the electronic and vibrational operators [10], can be used to convert the general Hamiltonian representing a strain in any direction into a Hamiltonian for a strain in a specific direction. This equivalence is lost when higher-order couplings are considered, and strains in different directions need to be considered explicitly.

In units in which the reduced mass of the mode, the mode frequency and $\hbar$ are set to unity, the components of $\mathcal{H}$ can therefore be written in the form

$$\begin{aligned} \mathcal{H}_{\text{int}} &= k \sum_\nu Q_\nu \sigma_\nu \\ \mathcal{H}_{\text{vib}} &= \tfrac{1}{2} \sum_\nu \left(P_\nu^2 + Q_\nu^2 \right) \\ \mathcal{H}_{\text{strain}} &= -w \sigma_\theta \end{aligned} \tag{2}$$

where ν is summed over all of the components of the vibrational mode. The $P_\nu = -\mathrm{i}\partial/\partial Q_\nu$ are the momenta conjugate to the Q_ν, k is the JT coupling constant for this system and w (which can be positive or negative) determines the strength of the strain. The σ_ν are electronic operators, which are expressed in the form of 8×8 matrices in [16] and [17], noting that our

coupling constant k is equivalent to $\sqrt{3}k$ in their papers as their k is the coupling constant for the $T \otimes$ h JT system applicable to C_{60}^{-}.

$\mathcal{H}_{\text{term}}$ is taken to be a matrix with values δ on its first three diagonal elements and all other values zero, such that a positive value for δ places the ^{2}P term above the ^{2}D term. Recent calculations indicate that the ^{2}P term is around 0.191 eV above the ^{2}D term [28]. It is useful to rewrite this in terms of the vibrational quantum $\hbar\omega$ for the effective mode under consideration. It is not clear what effective frequency should be used for C_{60}^{3-} ions. However, in the T_{2g} excited state of neutral C_{60}, the lowest-frequency h_g mode (at around 260 cm^{-1}) appears to be the one that is most strongly coupled [29], whilst the next-lowest mode at around 437 cm^{-1} is most strongly coupled for the ground state of C_{60}^{-} [3–5]. This suggests a value for δ of approximately $5.9\hbar\omega$. We will therefore use this value of δ when we plot our final graphs, although the results themselves will be formulated to apply for any value of δ.

3. Separation into vibrational and rotational motion

The first step is to examine the potential energy terms to determine the structure of the APESs around which the motion of the system will be based. When the JT effects experienced by an unstrained C_{60}^{3-} ion were considered previously, it was possible to separate the vibrational and pseudo-rotational motions by re-parametrizing the Q_ν in terms of a radial coordinate Q and four angles, θ, ϕ, γ and α [16, 17]. θ, ϕ and γ correspond to the usual Euler angles and α fixes the orientation of the coordinate system. To ensure that all points in the five-dimensional space are covered only once, it is necessary to impose the restrictions such as $0 \leqslant \alpha < \pi/3$, $0 \leqslant \gamma < \pi$, $0 \leqslant \theta < \pi/2$ and $0 \leqslant \phi < 2\pi$. A series of rotations in each of the four angles then reduces the potential to a form involving the angle α and the term splitting δ only [16, 17]. As the result is independent of the angles θ, ϕ and γ, they are free to take any values (within their range of definition). This means that the APES is a multi-dimensional trough of minimum-energy points a fixed distance Q from the origin. This specific value of Q will be defined to be the radius ρ of the trough. It therefore follows that the motion of the system at any one point on the lowest APES can be decomposed into vibrations in two directions in Q-space and pseudo-rotations in the other three directions (i.e. around the trough of minimum-energy points) [16, 17, 22]. Any one of six from the total of eight APESs can be made to be a minimum by a suitable choice of α. In [16] and [17], the choice $\alpha = \pi/2$ was made, even though this lies outside the range of definition, because (after some algebra) it can be seen that $\mathcal{H}_{\text{vib}}$ separates into a standard Hamiltonian for a two-dimensional vibration and a Hamiltonian for a form of symmetric top about the z-axis [16, 17]. The latter can be solved to gives the required three-dimensional pseudo-rotation.

An alternative method of separating the pseudo-rotational motion from that of the vibrations is to use rotating coordinates

$$Q'_\nu = \sum_\lambda D_{\nu\lambda}(\theta, \phi, \gamma, \alpha) Q_\lambda \tag{3}$$

where λ and ν take the values θ, ϵ, 4, 5 and 6, and the $D_{\nu\lambda}$ are rotation matrix elements. With the form of rotation matrix given in [23], at any given point on the trough the Q'_θ and Q'_ϵ modes correspond to vibrations and the Q'_4, Q'_5 and Q'_6 modes to rotations. This form of parametrization is useful as it properly identifies the local normal modes at any given point on the trough, which naturally separate into pseudo-rotations and vibrations. Therefore it is relatively easy to include anisotropic effects, for example, by assigning different frequencies to each of the Q'_ν normal modes.

When strain is included, either of the above methods can still be used to separate the vibrations and rotations. However, strain does not affect all of the six possible minimum

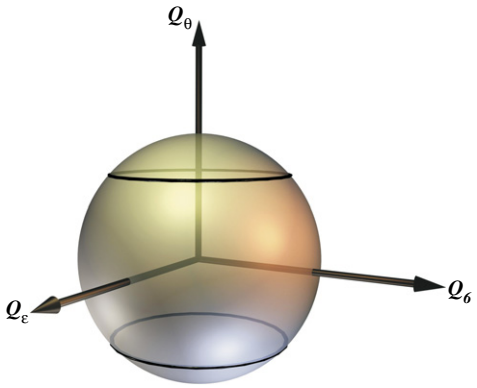

Figure 1. In the absence of any strain, the minimum-energy points on the lowest APES in the five-dimensional Q-space can be mapped onto the surface of a sphere in three dimensions. When a strain $-w\sigma_\theta$ is added in the Q_θ direction, the minimum points form a circle in the Q_ϵ–Q_6 plane, centred on $Q_\theta = -\frac{\sqrt{3}}{2}\rho$ for $w > 0$ and $Q_\theta = \frac{\sqrt{3}}{2}\rho$ for $w < 0$.

APESs in the same way. In particular, the lowest APES with $\alpha = \pi/2$ is unaffected by strain. Hence in [22] the choice $\alpha = \pi/6$ was made. This choice will be followed here. In the absence of strain, the vibrational Hamiltonian for this value of α can be separated into vibrational and rotational parts as with $\alpha = \pi/2$. However the Hamiltonian for the rotational part is now that of a symmetric top about the x-axis instead of the z-axis. When strain is included, the minimum-energy points no longer occur for all values of θ, ϕ and γ but only for $\theta = \gamma = \pi/2$ when the coefficient $w > 0$, and $\theta = 0$ when $w < 0$. There is now a circle of minimum-energy points of radius $\rho/2$ in the Q_ϵ–Q_6 plane, as shown in figure 1. When $w > 0$, the circle is centred on $Q_\theta = -\frac{\sqrt{3}}{2}\rho$ and the angle to the Q_ϵ-axis is 2ϕ. When $w < 0$, the circle is centred on $Q_\theta = \frac{\sqrt{3}}{2}\rho$ and the angle to the Q_ϵ-axis is $2(\phi + \gamma)$. In both cases, two of the modes that were rotations in the absence of strain have now been converted to vibrations. In terms of the rotating coordinates Q'_ν, setting $\theta = \pi/2$ and $\gamma = \pi/2$ (for $w > 0$), it can be seen that the Q'_4 and Q'_6 modes are converted to vibrations, leaving a pseudo-rotation around a circle of minimum-energy points in the Q'_5 direction only. When $\theta = 0$ (for $w < 0$), Q'_4 and Q'_5 are the vibrations and Q'_6 is the pseudo-rotation.

In terms of the radial coordinate Q, the energy of the minimum points on the lowest APES (for both signs of $|w|$) is

$$V = \tfrac{1}{2}\left(Q^2 + \delta - \sqrt{(2kQ + |w'|)^2 + \delta^2}\right) \tag{4}$$

where $w' = \sqrt{3}w$. When $w = 0$, this result is equivalent to the result obtained [22] for the unstrained $p^3 \otimes h$ system. The value of $Q \equiv \rho$ on the minimum-energy surface can be found by minimizing V with respect to Q. It can be seen that when the term splitting δ is zero, the radius is $\rho = k$. In general the radius is a root of the quartic equation

$$(Q^2 - k^2)(2kQ + |w'|)^2 + Q^2\delta^2 = 0 \tag{5}$$

which can easily be found numerically for any given values of k, w and δ. In fact, the numerical solutions when the JT coupling dominates over both the term splitting and the strain, i.e. for $k^2 > \delta$ and $k^2 > |w|$ are always very close to k. For example, the numerical solution for $k = 5$, $\delta = 5$ and $w = 5$ (which represents quite a large strain and term splitting) is $\rho = 4.98182$, which differs from $k = 5$ by only 0.36%. One other point of note, which we will revisit later,

is that when the term splitting is large compared to the JT coupling and strain, the radius of the trough is zero meaning the potential energy surface is simply a point at the origin. A similar result was noted previously in [30].

4. The wavefunction

From this point, we will mostly give results for the case when $w > 0$, although it is a simple matter to adapt our results for the $w < 0$ case, mostly just by changing some signs in relevant definitions. The complete wavefunction for a general state of the system with p, q, r and s excitations of θ', ϵ', $4'$ and $6'$ symmetries respectively (for $w > 0$), and with rotational quantum number m, will be written in the form $|\psi_{\rm tot};\ p, q, r, s, m\rangle$. We will now seek an algebraic form for this wavefunction that takes into account the coupled electronic, vibrational and rotational motion of the system.

4.1. Glauber state

If the electronic, rotational and vibrational wavefunctions at any point on the lowest APES are written as $\psi_{\rm g}$, $\psi_{\rm rot}(m)$ and $\psi_{\rm vib}(p, q, r, s)$ respectively, we can intuitively see that the total wavefunction must be able to be written as an integral

$$|\psi_{\rm tot};\ p, q, r, s, m\rangle = \int_0^{2\pi} \psi_{\rm g}\psi_{\rm rot}(m)\psi_{\rm vib}(p, q, r, s)\,{\rm d}\phi \tag{6}$$

over the circle of minimum-energy points on the lowest APES defined by the angle ϕ. The fact that $\psi_{\rm g}$, $\psi_{\rm rot}(m)$ and $\psi_{\rm vib}(p, q, r, s)$ are inside the integral reflects the fact that the three types of motion cannot be separated. It is also possible to derive this result formally using projection operator methods, which allow a state with the correct overall symmetry to be projected out from knowledge of one point on the minimum-energy surface only. The projection operator method follows general ideas first presented by Judd [32], and then further developed for the $T \otimes d$ [33, 34] and $E \otimes e$ [35] JT systems, where states of the form of equation (6) were referred to as Glauber states. These are coherent states of a harmonic oscillator. Glauber states are more commonly used to describe a wave pulse which oscillates back and forth across a potential well retaining its shape over time (and which can be used to model a continuous wave laser field or an electromagnetic field of unmodulated radio wave, for example). They have however been used in a JT context to analyse various specific JT systems [36, 37]. Although Glauber states have a well-defined physical meaning, they are not eigenstates of the harmonic oscillator problem. (In fact, they are eigenstates of phonon annihilation operators.) In the current context, the Glauber states describe the pseudo-rotation of the distortion around the minimum-energy trough (as well as vibrations 'across' the trough). We will refer back to this point when discussing the forms of $\psi_{\rm vib}$ and $\psi_{\rm rot}$. Full details of the projection operator approach were given for the $T \otimes {\rm h}$ JT system (applicable to C_{60}^-) in [31] so will not be repeated here.

We now require more specific forms for $\psi_{\rm g}$, $\psi_{\rm vib}$ and $\psi_{\rm rot}$ in order to evaluate the allowed energies of the system. From diagonalization of the interaction Hamiltonian $\mathcal{H}_{\rm int}$, the electronic wavefunction on the lowest APES with the angles and electronic basis defined as above can be seen to be

$$\psi_{\rm g} = \tfrac{1}{2}\left\{-\sqrt{2-\delta'}\sin\phi, \sqrt{2-\delta'}\cos\phi, 0, 0, \sqrt{2+\delta'}\cos\phi, 0, 0, \sqrt{2+\delta'}\sin\phi\right\} \tag{7}$$

where

$$\delta' = \frac{2\rho\delta}{k(w' + 2k\rho)}. \tag{8}$$

For the JT state to exist, it is necessary to have $\delta' < 2$ ($\delta' > 2$ is predominantly not a JT problem, so is not considered further here). This leads to the condition referred to in section 3 that the trough of minimum-energy points does not exist if the term splitting is large compared to the JT coupling. For given values of δ and w, this means there is a minimum value of $k \equiv k_{\min}$ for which results can be obtained. This minimum value can be found by solving the equation $\delta' = 2$ numerically. Alternatively, if we make the assumption that $\rho \approx k$, the value is $k_{\min} = \sqrt{(\delta - w')/2}$ for $\delta > w'$ and $k_{\min} = 0$ for $\delta < w'$. In addition to the condition on δ', is also necessary to choose values for k, w and δ such that the frequencies $\lambda_{\nu'}$ all remain real. For typical values, this will not introduce any extra conditions.

The Hamiltonian for the rotational part of the kinetic energy (i.e. the part of $\mathcal{H}_{\text{vib}}$ involving the momentum of the rotational mode) can be found from the symmetric top Hamiltonian appropriate for the unstrained case [16, 17] after substitution of $\alpha = \pi/6$ and $\theta = \gamma = \pi/2$, giving a contribution proportional to $\partial^2/\partial\phi^2$. Eigenfunctions of this operator are simply

$$\psi_{\text{rot}}(m) = \mathrm{e}^{\mathrm{i}m\phi}. \tag{9}$$

Clearly m must be an integer for the wavefunction to be invariant under the transformation $\phi \to \phi + 2\pi$. It is later found that for the overall state to exist, m must be an odd integer. Alternatively, the same results can be found by restricting the angles in the symmetric top wavefunctions obtained in [22] for the unstrained $p^3 \otimes h$ problem. The results are exactly as we would expect physically for rotation around a circle, where eigenfunctions are eigenstates of an angular momentum operator $\hat{l}_z = \mathrm{i}\hbar\partial/\partial\phi$, and is also the same as for the more familiar $E \otimes e$ JT problem where rotation is also around a circle at the bottom of the so-called 'Mexican hat' potential.

Although the $\psi_{\text{rot}}(m)$ are angular momentum eigenfunctions, they are not the most appropriate functions for describing the motion of a JT system because they do not represent localized functions. A physical distortion of a (fullerene) molecule must be localized, and is therefore more appropriately described by a localized function. Just as a plane-wave $\mathrm{e}^{\mathrm{i}kx}$ must be multiplied by a Gaussian-type function in x to localize it into a coherent pulse, it is necessary to multiply $\mathrm{e}^{\mathrm{i}m\phi}$ by an appropriate Gaussian in the rotational coordinate to represent the situation in which there is a localized distortion at any given instant. The direction of the distortion will then rotate in time, without changing the overall shape of the distortion. Pictures illustrating the pseudo-rotation of a distortion are given in [17]. However, as the ground state of a simple harmonic oscillator is a Gaussian function, the extra factor required to localize the rotation can be introduced by counting it in the *vibrational* wavefunction. Thus it will appear that our wavefunction contains a contribution from the ground state of a harmonic oscillator in the Q'_5 coordinate, although the presence of this term is to give a correct rotational wavefunction. Note that this does not mean that we should consider states with phonon excitations in Q'_5, because the term is not representing a vibration. It should also be noted that a term equivalent to that in Q'_5 is implicitly present in previous work on other systems that used Glauber-type states [35, 22, 23], where results of analytical calculations agree well with those of numerical methods. However, its presence was hidden through use of second-quantized notation.

4.2. Anisotropic effects

As stated in section 3, the four vibrations will have different frequencies, with the frequencies in the directions that are pseudo-rotations in the absence of strain being much lower than

those in the Q'_θ and Q'_ϵ directions that are always vibrations. In fact, we will show that the frequency of the Q'_ϵ modes is identically equal to ω and that of the Q'_θ mode is very close to ω (such that neglecting the difference from ω does not make very much difference to the overall results). However, Q'_4 and either Q'_6 for $w > 0$ or Q'_5 for $w < 0$ are rotations in zero strain and vibrations in finite strain. Therefore for weaker strains the potential barriers in these two directions will be much lower than those in the Q'_θ and Q'_ϵ directions. This anisotropy is important for all values of strain. We will now consider this anisotropy in more detail.

In previous work, anisotropy has been incorporated into JT problems in two ways. In strong 'coupling', which means both strong JT coupling and strong strain in the current context, it is possible to expand the potential about a minimum point on the trough of minimum-energy points to second order and diagonalize the resultant matrix M. The eigenvalues are the squares of the anisotropic frequencies for each of the Q'_ν modes [39]. The degeneracies of the frequencies agree with those predicted by group theory for the appropriate symmetry of the minimum (which is lower than I_h). Analysis of the corresponding eigenvectors allows symmetry labels to be assigned to the resulting frequencies. In fact, the curvature matrix

$$S = \begin{pmatrix} -\frac{\sqrt{3}}{2} & \frac{1}{2}\cos 2\phi & 0 & 0 & \frac{1}{2}\sin 2\phi \\ -\frac{1}{2} & -\frac{\sqrt{3}}{2}\cos 2\phi & 0 & 0 & -\frac{\sqrt{3}}{2}\sin 2\phi \\ 0 & 0 & \sin\phi & \cos\phi & 0 \\ 0 & -\sin 2\phi & 0 & 0 & \cos 2\phi \\ 0 & 0 & \cos\phi & -\sin\phi & 0 \end{pmatrix}, \tag{10}$$

(for $w > 0$) whose rows are the components of the Q_ν necessary to define the Q'_ν on the minimum-energy surface, will automatically diagonalize M via the operation $S \cdot M \cdot S^\dagger$ and results in the anisotropic frequencies labelled in terms of the Q'_ν modes automatically [40]. It is found convenient to write the frequencies in the form $\omega_{\nu'} = \lambda_{\nu'}\omega$. For the strained $p^3 \otimes h$ problem, this method of calculation gives

$$\begin{aligned} \lambda_{\theta'} &= \sqrt{1 - \frac{2\delta^2\rho^3}{k(w' + 2k\rho)^3}} \\ \lambda_{\epsilon'} &= 1 \\ \lambda_{4'} &= \sqrt{1 - \frac{2k\rho}{(w' + 2k\rho)}} \\ \lambda_{5'} &= 0 \\ \lambda_{6'} &= \sqrt{1 - \frac{k\rho}{(w' + k\rho)}}. \end{aligned} \tag{11}$$

$\lambda_{\epsilon'} = 1$ shows that the frequency of the vibration in the Q'_ϵ direction is unaltered by the strain. The $\lambda_{5'} = 0$ corresponds to the pseudo-rotation in the Q'_5 direction, but does not give the Gaussian term that is required to localize the rotational distortion. $\lambda_{4'}$ and $\lambda_{6'}$ both tend to 1 when the strain is much larger than the vibronic coupling, and decrease towards zero when the strain is small compared to the vibronic coupling. This is the required behaviour to describe the conversion of a vibration to a pseudo-rotation as the magnitude of the strain is decreased. It can be seen that these two frequencies are very similar to each other. The remaining frequency, $\lambda_{\theta'}$, tends to one in large strains, and is identically equal to one when the term splitting δ is zero.

An alternative approach to anisotropy, which extends the strong-coupling results to weaker strains, is to first apply a shift transformation

$$U_d = \exp\left(\frac{\alpha_\theta}{\sqrt{2}}(b'^\dagger_\theta - b'_\theta)\right), \tag{12}$$

where α_θ is a variational parameter, and $b_\theta'^\dagger$ and b_θ' are phonon creation and annihilation operators respectively for the θ' mode. The shift transformation has the effect of shifting the origin of coordinate Q_θ' to $Q_\theta' - \alpha_\theta$ (and leaving the origin of each of the other vibrational modes unaltered). Thus if the value of α_θ is set to the radius of the trough ρ, the origin is shifted to a minimum-energy point on the APES. (This can be confirmed using the Öpik–Pryce method.) The overall effect on the Hamiltonian is that it can be divided into a part that does not contain phonon operators and a part that does. The latter represents higher-order terms and so can be neglected for the current purposes. Note that the wavefunction at this stage can be compared directly with the usual form given for Glauber coherent states [35] as, due to the commutation properties of the $b_\nu^\dagger$ and b_ν,

$$U_{\rm d}\psi_{\rm vib}(p,q,r,s) \equiv {\rm e}^{\kappa(b_\theta'^\dagger - b_\theta)}\,|0\rangle = {\rm e}^{-\frac{1}{2}\kappa^2}{\rm e}^{\kappa b_\theta'^\dagger}(b_\theta'^\dagger - \kappa)^p (b_\epsilon'^\dagger)^q (b_4'^\dagger)^r (b_6'^\dagger)^s\,|0\rangle \tag{13}$$

where $\kappa = \rho/\sqrt{2}$.

Secondly, a scale transformation

$$U_{\rm s} = \exp\left(\sum_{\mu\nu}\Lambda_{\mu\nu}(b_\mu b_\nu - b_\mu^\dagger b_\nu^\dagger)\right) \tag{14}$$

is applied to rescale the coordinates Q_ν. The sum is over μ and $\nu = \theta$ and ϵ with $b_\epsilon^\dagger$ and b_ϵ defined in a similar manner $b_\theta^\dagger$ and b_θ. The $\Lambda_{\mu\nu}$ are parameters which form a matrix Λ whose values can be fixed by minimizing the energy of the ground state at a minimum-energy point calculated to second order in perturbation theory [39–42]. The effect of $U_{\rm s}$ is to scale the Q_ν according to the relation

$$U_{\rm s}^\dagger Q_\nu U_{\rm s} = \sum_\mu {\rm e}^{-2\Lambda}_{\mu\nu} Q_\mu \tag{15}$$

where the ${\rm e}^{-2\Lambda}_{\mu\nu}$ are elements of a matrix ${\rm e}^{-2\Lambda}$ defined in terms of the matrix Λ as a power series expansion. The effect on a harmonic oscillator-like function for vibrational modes Q_ν of frequency ω (in units in which the reduced mass and $\hbar$ are set to 1) is thus [42]

$$\exp\left(-\tfrac{1}{2}\sum_\mu \omega Q_\mu^2\right) \to \exp\left(-\tfrac{1}{2}\sum_\mu \omega_{\mu'} Q_\mu'^2\right) \tag{16}$$

where the Q_μ' are the local mode coordinates in equation (3) and the $\omega_{\mu'}$ are the corresponding frequencies. This result is of the required form for an anisotropic oscillator.

Mathematically, it is found that the required form for the matrix Λ is given by

$$\Lambda = \tfrac{1}{4} S^\dagger \cdot [\ln(\lambda_{\nu'})] \cdot S \tag{17}$$

where $[\ln(\lambda_{\nu'})]$ is a diagonal matrix with diagonal elements $\ln(\lambda_{\nu'})$. It is then found that

$$\begin{aligned}
\lambda_{\theta'} &= \sqrt{1 - \frac{2\delta^2\rho^3}{[k(w'+2k\rho)+\rho](w'+2k\rho)^2}} \\
\lambda_{\epsilon'} &= 1 \\
\lambda_{4'} &= \sqrt{1 - \frac{2k\rho[k(w'+2k\rho)-\delta\rho]}{(w'+2k\rho)[k(w'+2k\rho)+\rho(2-\delta)]}} \\
\lambda_{5'} &= 1 \\
\lambda_{6'} &= \sqrt{1 - \frac{k\rho[\rho(w'+3k\rho)+2k]}{\rho(w'+3k\rho)(w'+k\rho)+4(\rho+kw'+2k^2\rho)}}.
\end{aligned} \tag{18}$$

These results reduce to the expressions given in equation (11) in strong coupling and strong strain (i.e. $k \gg 1$, $\rho \gg 1$ and $w \gg 1$ in units of $\hbar\omega$), except for the rotational mode Q_5'.

The simpler strong-'coupling' (i.e. strain) method gave $\lambda_{5'} = 0$, which does not allow for the localization of the rotational state. This method automatically gives a value that is appropriate for producing a coherent state.

4.3. Vibrational wavefunction and normalization of total wavefunction

In terms of the scale transformation parameters, the (unnormalized) ground-state 'vibrational' wavefunction at a point on the trough including anisotropy and the term to localize the vibrational function can be written (in units $\hbar = 1$) in the general matrix form [42]

$$\psi_{\rm vib}(0,0,0,0) = {\rm e}^{-\frac{1}{2}[\vec{Q}+\vec{\alpha}]^{\dagger}\cdot{\rm e}^{4\Lambda}\cdot[\vec{Q}+\vec{\alpha}]} \tag{19}$$

where $\vec{Q} = (Q_\theta, Q_\epsilon, Q_4, Q_5, Q_6)$. $\vec{\alpha}$ is a vector with components α_γ characterizing the positions of the bottom of the trough. The form for $\vec{\alpha}$ in this case is

$$\vec{\alpha} = \left(\frac{\sqrt{3}}{2}\rho, -\frac{\rho}{2}\cos 2\phi, 0, 0, -\frac{\rho}{2}\sin 2\phi\right). \tag{20}$$

From the definition of the matrix Λ in equation (17), it follows that ${\rm e}^{4\Lambda}$ is given by the matrix

$${\rm e}^{4\Lambda} = S^{\dagger}\cdot[\lambda_{\nu'}]\cdot S, \tag{21}$$

where $[\lambda_{\nu'}]$ is a diagonal matrix with elements $\lambda_{\nu'}$. For the case here (with $w > 0$), this gives

$$\psi_{\rm vib}(0,0,0,0) = {\rm e}^{-\frac{1}{2}[\lambda_{\theta'}(Q'_\theta-\rho)^2+Q'^2_\epsilon+\lambda_{4'}Q'^2_4+Q'^2_5+\lambda_{6'}Q'^2_6]}. \tag{22}$$

It can thus be seen that the scale transformation has had the required effect. This is exactly of the form expected for a vibration in the Q'_θ direction centred on $Q'_\theta = \rho$ of frequency $\lambda_{\theta'}\omega$ and vibrations centred on the origin in the Q'_ϵ, Q'_4 and Q'_6 directions with frequencies ω, $\lambda_{4'}\omega$ and $\lambda_{6'}\omega$ respectively, combined with the Gaussian term in Q'_5 to localize the rotational wavefunction and produce a coherent state.

We now have an explicit analytical expression for the complete states $|\psi_{\rm tot};0,0,0,0,m\rangle$ with no vibrational excitations, but they must be normalized. This can be accomplished by converting the Q'_ν to Q_ν using equation (3) and integrating the overlap of the wavefunction at a point ϕ with the wavefunction at ϕ' over all of the Q_ν (which can be done analytically using standard integral results), then integrating over $\phi + \phi'$. Finally this leaves the single integral over $y = \phi - \phi'$,

$$O^m_{\rm tot} \equiv \langle\psi_{\rm tot};0,0,0,0,m|\psi_{\rm tot};0,0,0,0,m\rangle = F(1,m), \tag{23}$$

where

$$F(f,m) = 32\sqrt{2}\pi^{7/2}{\rm e}^{-\lambda_\theta\rho^2}\int_0^{2\pi}\frac{f{\rm e}^{\frac{\rho^2\lambda^2_{\theta'}}{Y}(7+\cos 2y)}\cos y\cos my}{\sqrt{XYZ}}\,{\rm d}y \tag{24}$$

with

$$\begin{aligned} X &= 7+\lambda_{\theta'}-(-1+\lambda_{\theta'})\cos 2y \\ Y &= 1+7\lambda_{\theta'}+(-1+\lambda_{\theta'})\cos 2y \\ Z &= \lambda^2_{4'}+6\lambda_{4'}\lambda_{6'}+\lambda^2_{6'}-(\lambda_{4'}-\lambda_{6'})^2\cos 2y. \end{aligned} \tag{25}$$

It is not surprising that the final result is a single integral as all points on the trough are equivalent, and so the overlap between two points on the trough can depend only on the angular difference in the positions of the two points. It is a simple matter to evaluate the integral in $O^m_{\rm tot}$ numerically for any values of k, w and δ, noting that m must be an odd integer as stated below equation (9). The symmetry of the function to be integrate is such that if m

is taken to be even, the overlap integrals are all zero. It should also be noted that, as we will discuss further in section 5.2, the integrals become those defining Bessel functions in the limit of no anisotropy ($\lambda_{\theta'} = \lambda_{4'} = \lambda_{6'} = 1$ and thus $X = Y = Z = 8$).

Although the above results are for $w > 0$, results for $w < 0$ can be obtained by replacing ϕ by $z = \phi + \gamma$ and changing some signs in subsequent formula. For example, the electronic ground state equivalent to equation (7) is

$$\psi_g = \tfrac{1}{2}\left\{\sqrt{2-\delta'}\cos z, \sqrt{2-\delta'}\sin z, 0, 0, -\sqrt{2+\delta'}\sin z, 0, 0, \sqrt{2+\delta'}\cos z\right\}. \tag{26}$$

5. Energy calculation

5.1. Results including anisotropy

In previous papers that included anisotropy via the scale transformation, it was found that the energy of the states with no vibrational excitations should be calculated using a wavefunction equivalent to equation (19) corrected to second order in perturbation theory via coupling to phonon excited states on the upper APES sheets [42]. Second-order corrections to the states are necessary because the anisotropic corrections to the energy are second order. If the states are only taken to first order, the energies of the minimum points can be raised rather than lowered by anisotropy, which is incorrect as the scale transformation is a variational method. However, the formulae incorporating the scale transformation to second order are rather complicated, and no attempt has been made to incorporate such corrections to states with phonon excitations. An additional problem occurs in the current problem where there is a trough on the lowest APES. We will take an alternative approach here. Results including the second-order corrections on previous systems, such as the cubic $E \otimes e$ system, are equivalent to those taking the zeroth-order wavefunction only but including the anisotropic frequencies $\lambda_{\nu'}$ in the vibrational Hamiltonian. This is not surprising as the desired effect of including anisotropy is to make the system appear as if it is composed of harmonic oscillators of (dimensionless) frequency $\lambda_{\nu'}$. Therefore, for our current problem we will use the vibrational Hamiltonian

$$\mathcal{H}_{\text{vib}} = \tfrac{1}{2}\sum_{\nu}\left(P_\nu^2 + \lambda_{\nu'}^2 Q_\nu'^2\right) \tag{27}$$

(noting that the second term must be written in terms of the rotating (primed) coordinates but the first term need not be as $\sum_\nu P_\nu'^2 = \sum_\nu P_\nu^2$). The matrix elements of $\mathcal{H}$ are now determined in a similar manner to the overlap. The energies are calculated in terms of the energy E_g of the ground state in strong coupling given by

$$E_g = -E_{JT} + \tfrac{1}{2}\left(\lambda_{\theta'} + \lambda_{\epsilon'} + \lambda_{4'} + \lambda_{6'}\right). \tag{28}$$

E_{JT} refers to the terms

$$E_{JT} = \frac{\lambda_{\theta'}^2\rho^2}{2} + \frac{w}{2}\frac{\rho}{k} - \frac{\delta}{4}(2-\delta'). \tag{29}$$

The first term in E_{JT} is equivalent to the usual JT energy due to the vibronic coupling, and the remaining two terms are from the strain and term splitting respectively. The remaining terms in E_g give the zero-point energy for the four vibrational modes. Note that although it was necessary to include a term in $\lambda_{5'}$ to localize the rotation, it is not necessary to include a zero-point energy contribution of $\frac{1}{2}\lambda_{5'}$ for this mode, which is to be expected as it is a rotation not a vibration.

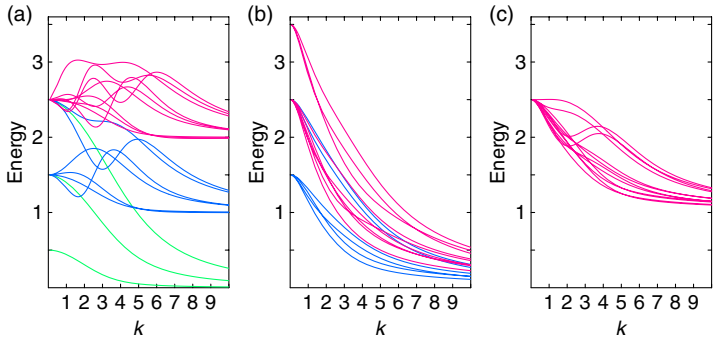

Figure 2. Energies of states with up to three rotational excitations and two vibrational excitations (including anisotropic effects), as a function of the JT coupling k and in units of $\hbar\omega$. The results are calculated with $w = 0$ and $\delta = 0$ and plotted relative to E_g. In subplot (a), the three states with lowest energy in strong coupling (green lines) are those of the states with no phonon excitations, the next six states (blue lines) are states with one-phonon excitation of type θ' or ϵ' and the remaining states are those that have two-phonon excitations of type θ' and/or ϵ'. Subplot (b) includes similar states as for (a) but with $4'$ and/or $6'$ excitations, and (c) is for one θ' or ϵ' excitation and one $4'$ or $6'$ excitation.

A relatively simple calculation shows that the energy of the states with no vibrational excitations in finite coupling can be written in the form

$$E_0^m = E_g + \frac{M_{\rm int}^m + M_{\rm vib}^m}{O_{\rm tot}^m} \tag{30}$$

where $M_{\rm int}$ and $M_{\rm vib}$ are matrix elements from the interaction and vibrational terms respectively given by

$$\begin{aligned} M_{\rm int}^m &= F\left(-\frac{8\rho^2\lambda_{\theta'}}{Y}, m\right) \\ M_{\rm vib}^m &= F\left(\frac{\rho^2\lambda_{\theta'}^3}{Y}(7+\cos 2y), m\right). \end{aligned} \tag{31}$$

Having obtained a result for the anisotropic ground states, we can now move on to consider excited vibrational states with p, q, r and s excitations of the Q'_θ, Q'_ϵ, Q'_4 and Q'_6 oscillators respectively. In principle, these could have been considered with the scale transformation approach by including appropriate creation operators, but as stated previously the mathematics soon becomes prohibitively complicated. It is a much simpler matter to extend the calculations to the excited states in the coordinate representation, simply by including appropriate Hermite polynomials in the states in $\psi_{\rm vib}$. The integrals over the Q_ν can still be performed analytically and the overall results reduced to a single integral over y. One unusual feature is that, since Q'_4 and Q'_5 contain factors $\cos\phi$ and $\sin\phi$, m must be even when $r + s$ is odd, and odd when $r + s$ is even in order for the overall parity of the wavefunction to be conserved.

We will first calculate the energies of states for the case when $w = 0$ and $\delta = 0$. Although the results are not strictly valid when $w = 0$ as the lowest potential surface consists of a three-dimensional trough and not a one-dimensional one as modelled here, it is still useful to plot this case for illustration purposes. In previous papers, it has been found to be convenient to plot the results obtained relative to the constant energy $E_{\rm JT}$. However, in this problem, it will be more informative to plot the results relative to E_g. This is because when strain is included and the term splitting $\delta = 0$, the only dependence of some of the results on the strain w is through the zero-point energy. Results with up to two-phonon excitations and three rotational excitations are shown in figure 2 as follows. The three curves on subplot (a) with lowest energy in strong

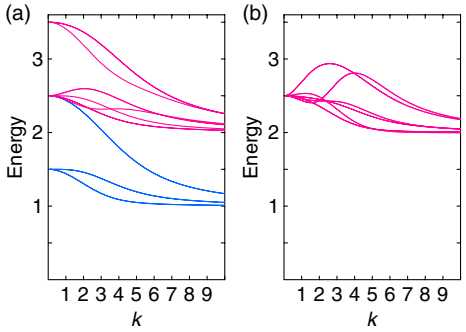

Figure 3. As subplots (b) and (c) of figure 2 but neglecting anisotropic effects.

coupling give the energy of the lowest three rotational states with no phonon excitations. When plotted relative to E_g, these states tend to the expected energy limit of zero in strong coupling. The remaining curves in subplot (a) show states with θ' and/or ϵ' excitations. The energies clearly separate into bands in strong coupling according to the number of phonon excitations present. This is because the frequency $\lambda_{\epsilon'}$ is always identically equal to 1 and the frequency $\lambda_{\theta'}$ equals 1 in this limit of zero term splitting. Some of the excited states do not tend to the correct limits in weak coupling. This is because the model used does not work well in weak coupling, where the potential energy surface does not contain clearly defined wells. Non-orthogonality between states with the same rotational quantum number m also becomes important in this limit. An orthogonalization procedure can be used to improve the results, but this only has a significant effect in weak coupling and it makes the method considerably more complicated. Alternative numerical methods are more appropriate in this limit.

Subplot (b) of figure 2 shows states with $4'$ and/or $6'$ excitations, and (c) shows states with one θ' or ϵ' excitation and one $4'$ or $6'$ excitation. A separation into bands is not seen, with the energies of all the states merging in strong coupling. This is because the anisotropic frequencies $\lambda_{4'}$ and $\lambda_{6'}$ are very small (as the vibronic coupling dominates the strain) and so the separations between excited phonon states are also small.

Figure 3 shows results equivalent to subplots (b) and (c) of figure 2 but with the anisotropic frequencies $\lambda_{\nu'}$ all set to 1. The curves equivalent to subplot (a) are not given because they are identical to those in figure 3 when plotted relative to E_g. However it should be noted that energy of the states relative to the bottom of the trough (given by E_g) is rather higher than that obtained when anisotropy is not included. Subplot (b) shows a clear separation into energy bands in strong coupling according to the phonon occupation number. Both subplots show much less difference between the energy values in strong and weak coupling than with anisotropy, which is because the zero-point energies are much larger. The issue of incorrect limits in weak coupling still applies to these results. It should also be noted that there are accidental degeneracies between states with Q'_4 and Q'_6 excitations. This is because the frequencies of the modes are equal in the isotropic limit.

We will now look at the cases where there is a non-zero term splitting δ and/or strain term w. When a non-zero strain term ($w > 0$) is included but the term splitting remains zero, the levels with θ' and/or ϵ' excitations are identical to those in subplot (a) of figure 2 with $w = 0$. Again, the only absolute difference is in the energy E_g. The remaining results are very similar to those in subplots (b) and (c) of figure 2, having the same limits in strong and weak coupling. However, the energies reduce more slowly as the coupling strength increases, so that they do not reach their strong-coupling limits until larger values of k.

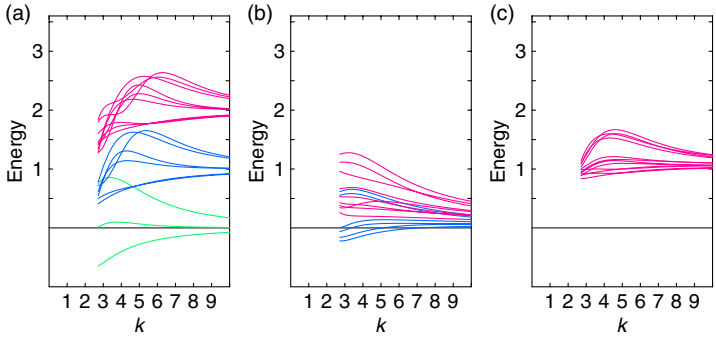

Figure 4. As figure 2 but with $\delta = 5.9$ in units of $\hbar\omega$.

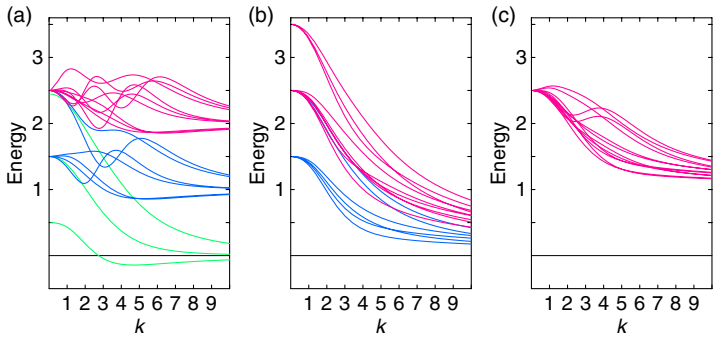

Figure 5. As figure 2 but with $w' = 10$ and $\delta = 5.9$ in units of $\hbar\omega$.

When the term splitting δ is non-zero, we can only obtain results for $k > k_{\min}$, as discussed in section 4. When $w = 0$, the results in strong coupling (relative to E_g) are very similar to those with no term splitting. This is shown in figure 4 for $\delta = 5.9$. In weaker coupling, as k reduces towards $k_{\min}$, the curves bend noticeably downwards. This is probably attributable to the fact that the states are becoming invalid in this limit. The issue does not arise when a relatively large strain is included as well as a non-zero term splitting, as $k_{\min}$ is again zero. Figure 5 shows results for $\delta = 5.9$ and $w' = 10$ (in units of $\hbar\omega$). Whilst the energy of the lowest curve on subplot (a) is now less than E_g, the general shape of all the curves is very similar to that in figure 2 where $w = \delta = 0$. Whilst the energies of the states themselves are altered by finite values of strain w and term splitting δ, we can conclude that almost all of the effect is in the 'constant' energy term E_g that is common to all of the states, unless the term splitting is large compared to both the JT coupling k and the strain.

5.2. Alternative calculation neglecting anisotropy

If anisotropy is neglected, the calculations become much simpler as all of the required integrals (for all ground and excited states) can be written in terms of integrals defining Bessel functions. This can be seen by setting $\lambda_{\theta'} = \lambda_{4'} = \lambda_{6'} = 1$ in the last section. Alternatively, the calculation can be carried out entirely in second-quantized form [43]. This makes the calculation for excited states in particular much simpler.

As a result of either of the above approaches, the overlap in equation (23) can be written in terms of sums of one-dimensional integrals of the form

$$\int_0^{2\pi} \cos(2ny) e^{-\frac{\rho^2}{8}(1-\cos 2y)}\, dy \equiv 2\pi e^{-\rho^2/8} I_n(\rho^2/8) \tag{32}$$

where n is an integer and $I_n(\rho^2/8)$ are modified Bessel functions of the first kind. Due to recursion relations between Bessel functions, the results can be written in a number of ways. The simplest form for the overlaps for the states with no phonon excitations and m up to 7 (with $I_n \equiv I_n(\rho^2/8)$) are

$$\begin{aligned} O^1_{\rm tot} &= \pi e^{-\rho^2/8}\,(I_0 + I_1) \\ O^3_{\rm tot} &= \pi e^{-\rho^2/8}\,(I_1 + I_2) \\ O^5_{\rm tot} &= \pi e^{-\rho^2/8}\,(I_2 + I_3) \\ O^7_{\rm tot} &= \pi e^{-\rho^2/8}\,(I_3 + I_4)\,. \end{aligned} \tag{33}$$

The energy levels can now be calculated by evaluating the matrix elements of $\mathcal{H}$ in a similar manner to the overlap factors [43]. It can be shown that the energies E_0^m of the states with no phonon excitations can be obtained from equation (30) by setting the $\lambda_{\nu'} = 1$, $M^m_{\rm int} = 0$ and

$$\begin{aligned} M^1_{\rm vib} &= \tfrac{1}{2}\pi e^{-\rho^2/8}\,(I_0 - I_1) \\ M^3_{\rm vib} &= \tfrac{3}{2}\pi e^{-\rho^2/8}\,(I_1 - I_2) \\ M^5_{\rm vib} &= \tfrac{5}{2}\pi e^{-\rho^2/8}\,(I_2 - I_3) \\ M^7_{\rm vib} &= \tfrac{7}{2}\pi e^{-\rho^2/8}\,(I_3 - I_4)\,. \end{aligned} \tag{34}$$

When the resulting energies are plotted, they are found to be identical to those for the no-phonon states obtained above (see subplot (a) of figure 2), which is to be expected as it is only the method of evaluation of the results that has changed. It should be noted that analytical results for states including phonon excitations can be obtained in a similar manner to that here, although they are more complicated (involving not only the Bessel functions but coefficients that depend upon ρ).

When anisotropic effects are neglected, the vibrations in the four vibrational directions all take place with the same frequency, so we could work with any linear combination of the Q_ν in these directions. This means that the separation into the Q'_ν used in equation (3) is more complicated than it need be. The much simpler set of coordinates $\{Q_\theta, Q_4, Q_5, Q_{\rm v}, Q_{\rm r}\}$ where $Q_{\rm r}$ is a rotational coordinate and $Q_{\rm v}$ is a vibrational coordinate, could be used in the absence of anisotropy. $Q_{\rm v}$ is equivalent to Q'_6 for $w > 0$ and Q'_5 for $w < 0$, and

$$Q_{\rm v} = Q_\epsilon \cos 2z + Q_6 \sin 2z \tag{35}$$

where $z = \phi$ for $w < 0$ and $z = \phi + \gamma$ for $w > 0$. However, the meaning of vibrational excitations is different with these new definitions and so the energies calculated are different from those obtained in section 5.2 for the limit of no anisotropy. Hence only the states with no vibrational excitations are directly comparable.

6. Expectation values

As mentioned in the introduction, dynamic distortions of an isolated molecule can become locked into static distortions in a solid due to cooperative vibronic interactions between molecules [7–9, 11, 12]. This can result in various different phases (structural, orientational, magnetic etc) depending on the exact nature of the JT couplings in any given solid, as discussed

in [10]. Determination of these coupling constants is beyond the scope of this paper. However, a signature of any cooperative phase will be that the expectation value $\langle Q_\nu \rangle$ of one or more of the Q_ν will be non-zero. However, the $\langle Q_\nu \rangle$ are proportional to the expectation values $\langle \sigma_\nu \rangle$ of the electronic operators σ_ν [15]. As the effect of the cooperative vibronic coupling can be modelled by a strain on an isolated molecule, we will now calculate these expectation values.

The expectation value of any operator $\mathcal{L}$ at temperature T can be defined as

$$\langle \mathcal{L} \rangle = \frac{\sum_i \langle \psi_i | \mathcal{L} | \psi_i \rangle \exp(-E_i/k_B T)}{\sum_i \exp(-E_i/k_B T)}. \tag{36}$$

The $|\psi_i\rangle$ are taken to be the complete set of (normalized) ground and excited vibronic states of the system, namely $|\psi_{tot};\, p, q, r, s, m\rangle$ in our case, the E_i are the corresponding energies and k_B is the Boltzmann constant.

In general, equation (36) can only be evaluated when the complete set of vibronic states is known. However, for the case of a strong θ-type strain, it is straightforward to show that $\langle \psi_{el} | \sigma_\lambda | \psi_{el} \rangle = 0$ for $\lambda = \epsilon$, 4, 5 and 6. The corresponding values of $\langle \sigma_\lambda \rangle$ are therefore zero. However, for $\lambda = \theta$,

$$\langle \psi_g | \sigma_\theta | \psi_g \rangle = \frac{\sqrt{3}\rho}{2k} \langle \psi_g | \psi_g \rangle. \tag{37}$$

Therefore, after substituting this result into the matrix element for the total state $|\psi_{tot};\, p, q, r, s, m\rangle$, integrating over all points on the trough and dividing by the overlap to normalize the state, the summations in the numerator and denominator of equation (36) cancel. This leaves the result

$$\langle \sigma_\theta \rangle = \frac{\sqrt{3}\rho}{2k}. \tag{38}$$

This tends to a constant value of $\sqrt{3}/2$ in strong strain (when $\rho = k$) and is still very close to $\sqrt{3}/2$ even in weaker strains due to the very weak dependence of ρ on w. The value is unaffected by anisotropy, because anisotropy only affects the vibrational component of the vibronic state, which drops out of this calculation.

$\langle Q_\theta \rangle$ can also be calculated directly from the vibronic states. The result should be proportional to that in equation (38) [15]. However, the calculated result is not exactly identical due to the fact that the analytical expressions used for the vibronic states are not exact. The matrix elements $\langle \psi_{tot};\, p, q, r, s, m | Q_\theta | \psi_{tot};\, p, q, r, s, m \rangle$ are not simply proportional to $\langle \psi_{tot};\, p, q, r, s, m | \psi_{tot};\, p, q, r, s, m \rangle$, so the summations in the numerator and denominator of the expression for $\langle Q_\theta \rangle$ do not cancel out. However, the contribution from the (normalized) ground state is exactly $-\frac{\sqrt{3}}{2}\rho$, and those for the excited states are very close to this value. From this we can conclude that $\langle Q_\theta \rangle \approx -k \langle \sigma_\theta \rangle$, showing that, to a good approximation, $\langle Q_\theta \rangle$ and $\langle \sigma_\theta \rangle$ are indeed proportional.

7. Conclusions

In this paper, we have used an analytical method to formulate states for the $p^3 \otimes h$ JT system subject to a strong strain. These states take into account the allowed vibrational and pseudo-rotational motion of the system around minimum points on the lowest APES, as well as the JT coupling between this motion and the motion of the electrons. The states can be used to determine the energies of this system by simple evaluation of one-dimensional integrals.

The results in this paper complement those obtained previously for an unstrained $p^3 \otimes h$ JT system [22]. It would be very interesting to consider the case of intermediate strains, which will link these two limiting cases, and in particular to evaluate $\langle \sigma_\theta \rangle$ over the complete range

of strains. However, it is not known in general how to formulate analytical wavefunctions for a hindered rotation, or how to track from a vibration in one limit to a rotation in another analytically. This can only be done in specific cases, such as the quadratic $E \otimes e$ problem where the rotational wavefunction can be replaced by Mathieu functions [9]. In other cases, it would be possible to either modify states for zero strain to apply with strain or modify the strong-strain states for weaker strains, but both of these approaches are difficult and the results would only be approximate. Another approach would be to solve the differential equation representing the motion in the coordinate(s) representing the hindered rotation(s) numerically and combine the results with the analytical results for the vibrational directions, in a similar manner to that used previously for the much simpler $E \otimes e$ problem. Alternatively, a numerical approach such as a Lanczos diagonalization could be used to obtain results for the problem as a whole in the intermediate strain region, although it would be very difficult to obtain a sufficiently large set of ground and excited states for the summations in equation (36) to converge. All such approaches are beyond the scope of this paper, as it is important to know results in the limit of strong strain before attempting to interpolate between weak and strong strain.

Although we do not have quantitative results for the intermediate strain region at this stage, it is nevertheless possible to make some qualitative predictions about $\langle \sigma_\theta \rangle$. We know from equation (38) that $\langle \sigma_\theta \rangle$ is approximately constant for strong strains. We also know that it must be zero when there is no strain, as this situation corresponds to a dynamic JT effect where distortions in equivalent symmetry directions are all equally likely. In the $E \otimes e$ system, the magnitude of $\langle \sigma_\theta \rangle$ was found to reduce smoothly from its strong-strain value until attaining the value of zero in no strain [15]. Also, the strong-coupling value is attained for much weaker strains at low temperatures than high ones. This seems reasonable as cooperative distortions are more likely to remain locked in place at low temperatures than high ones. Very similar qualitative behaviour is to be expected for the $p^3 \otimes h$ system.

It is hoped that the results in this paper will be useful in understanding the observed behaviour of fullerene solids such as the A_3C_{60} fullerides, in which C_{60}^{3-} ions can exhibit a $p^3 \otimes h$ JT effect with an overall effective strain due to coupling to intermolecular vibrational modes. In particular, the results may help the understanding of various structural and superconducting phase transitions in these solids.

References

[1] Wang W Z, Wang C L, Bishop A R, Yu L and Su Z B 1997 *Synth. Met.* **86** 2365
[2] Varma C M, Zaanen J and Raghavachari K 1991 *Science* **254** 989
[3] Breda N, Broglia R A, Colo G, Roman H E, Alasia F, Onida G, Ponomarev V and Vigezzi E 1998 *Chem. Phys. Lett.* **286** 350
[4] Gunnarsson O, Handschuh H, Bechthold P S, Kessler B, Gantefor G and Eberhardt W 1995 *Phys. Rev. Lett.* **74** 1875
[5] Alexandrov A S and Kabanov V V 1995 *Pis. Zh. Eksp. Teor. Fiz.* **62** 920
Alexandrov A S and Kabanov V V 1995 *JETP Lett.* **62** 937 (Engl. Transl.)
[6] Hands I D, Dunn J L and Bates C A 2001 *Phys. Rev.* B **63** 245414
[7] Kaplan M D and Vekhter B G 1995 *Cooperative Phenomena in Jahn–Teller Crystals* (New York: Plenum)
[8] Gehring G A and Gehring K A 1975 *Rep. Prog. Phys.* **38** 1
[9] Bersuker I B and Polinger V Z 1989 *Vibronic Interactions in Molecules and Crystals* (Berlin: Springer)
[10] Dunn J L 2004 *Phys. Rev.* B **69** 064303
[11] Kawamoto T and Suzuki N 1997 *Synth. Met.* **86** 2387
[12] Kawamoto T, Tokumoto M, Sakamoto H and Mizoguchi K 2001 *J. Phys. Soc. Japan* **70** 1892
[13] Kodama T, Kato M, Mogi K, Aoyagi M and Kato T 1997 *Mol. Phys. Rep.* **18/19** 121
[14] Kato T 2003 *Adv. Quantum Chem.* **44** 313
[15] Feiner L F 1982 *J. Phys. C: Solid State Phys.* **15** 1495
[16] O'Brien M C M 1996 *Phys. Rev.* B **53** 3775

[17] Chancey C C and O'Brien M C M 1997 *The Jahn–Teller Effect in* C_{60} *and Other Icosahedral Complexes* (Princeton, NJ: Princeton University Press)
[18] Gunnarsson O 1997 *Rev. Mod. Phys.* **69** 575
[19] Stephens P W, Mihaly L, Lee P L, Whetten R L, Huang S M, Kaner R, Deiderich F and Holczer K 1991 *Nature* **351** 632
[20] Auerbach A, Manini N and Tosatti E 1994 *Phys. Rev.* B **49** 12998
[21] Pooler D R 1980 *J. Phys. C: Solid State Phys.* **13** 1029
[22] Dunn J L and Li H 2005 *Phys. Rev.* B **71** at press
[23] Sookhun S, Dunn J L and Bates C A 2003 *Phys. Rev.* B **68** 235403
[24] Ceulemans A 1994 *Top. Curr. Chem.* **171** 27
[25] Choi C H, Kertesz M and Mihaly L 2000 *J. Phys. Chem.* A **104** 102
[26] O'Brien M C M 1983 *J. Phys. C: Solid State Phys.* **16** 6345
[27] Chibotaru L F 1994 *J. Phys. A: Math. Gen.* **27** 6919
[28] Nikolaev A V and Michel K H 2002 *J. Chem. Phys.* **117** 4761
[29] Negri F, Orlandi G and Zerbetto F 1988 *Chem. Phys. Lett.* **144** 31
[30] Borshch S A and Prassides K 1996 *J. Phys. Chem.* **100** 9348
[31] Dunn J L, Eccles M R, Liu Y M and Bates C A 2002 *Phys. Rev.* B **65** 115107
[32] Judd B R 1974 *Can. J. Phys.* **52** 999
[33] Judd B R and Vogel E E 1975 *Phys. Rev.* B **11** 2427
[34] Chancey C C 1987 *J. Phys. A: Math. Gen.* **20** 2753
[35] Chancey C C 1984 *J. Phys. A: Math. Gen.* **17** 3183
[36] Avram N M, Draganescu G E and Kibler M R 2002 *Int. J. Quantum Chem.* **88** 303
[37] Rivera-Iratchet J, Deorue M A, Flores M L and Vogel E E 1993 *Phys. Rev.* B **47** 10164
[38] Dunn J L and Eccles M R 2001 *Phys. Rev.* B **64** 195104
[39] Liu Y M, Dunn J L, Bates C A and Polinger V Z 1997 *J. Phys.: Condens. Matter* **9** 7119
[40] Qiu Q C, Dunn J L, Bates C A and Liu Y M 1998 *Phys. Rev.* B **58** 4406
[41] Liu Y M, Bates C A, Dunn J L and Polinger V Z 1996 *J. Phys.: Condens. Matter* **8** L523
[42] Dunn J L, Bates C A, Moate C P and Liu Y M 2003 *J. Phys.: Condens. Matter* **15** 5697
[43] Dunn J L 1988 *J. Phys. C: Solid State Phys.* **21** 383